

Persistent self-organized states in non-equilibrium magnetic models

R. A. Dumer* and M. Godoy†

*Programa de Pós-Graduação em Física, Instituto de Física,
Universidade Federal de Mato Grosso, Cuiabá, Brasil.*

In this work, we employed Monte Carlo simulations to study the Ising, XY , and Heisenberg models on a simple cubic lattice, where the system models evolve toward the steady state under the influence of competition between one- and two-spin flip dynamics. With probability q , the system is in contact with a thermal reservoir at temperature T and evolves toward the lower energy state through one-spin flip dynamics. On the other hand, with probability $1 - q$, the system is subjected to an external energy flux that drives it toward the higher energy state through two-spin flip dynamics. As a result, we constructed the phase diagram of T as a function of q . In this diagram, we identified the antiferromagnetic (AF) ordered phase, the ferromagnetic (F) ordered phase, and the disordered paramagnetic (P) phase for all the models studied. Through these phases, we observed self-organization phenomena in the systems. For low values of q , the system is in the AF phase, and as q increases the system continuously transitions to the P phase. Now, for high values of q , the system through continuous phase transitions again reaches an ordered phase, the F phase, at low values of T . Additionally, we also calculated the critical exponents of the system, showing that these are not affected by the non-equilibrium regime of the system.

I. INTRODUCTION

Magnetic models, such as Ising [1], Heisenberg [2], and XY [3], play a central role in statistical mechanics providing essential theoretical frameworks for studying phase transitions and critical behavior. In the Ising model, spins are restricted to a single axis, while in the XY model, they are confined to a plane. The Heisenberg model, in contrast, allows spins to adopt orientations in three dimensions. Despite their versatility, continuous models like XY and Heisenberg exhibit limitations in low dimensions, as established by the Mermin-Wagner theorem [4], which prohibits magnetic ordering in two dimensions for short-range interactions at finite temperatures. In higher dimensions, however, these constraints vanish, and these models display characteristic phase transitions.

Self-organization is a hallmark of many non-equilibrium systems, where macroscopic order emerges spontaneously from microscopic interactions without external coordination [5]. Examples include pattern formation in chemical reactions, such as the Belousov-Zhabotinsky reaction [6], biological systems like flocking in birds [7], cellular structures [8], and even traffic flow dynamics [9]. These systems demonstrate how competing processes and feedback mechanisms can drive the system toward ordered states or complex behaviors. In the context of magnetic systems, competition between different dynamics can also lead to self-organization, fostering the emergence of non-trivial steady states, which may exhibit transitions between different ordered phases [10–13].

In dealing with magnetic systems governed by competing dynamics, the principle of microscopic reversibility is not always satisfied, forcing the system out of equilibrium and beyond the scope of the formalism proposed by

Gibbs for thermodynamic equilibrium systems [14]. In this competition, one-spin flip and two-spin flip dynamics are frequently employed [15–18]. The one-spin flip dynamic, acting with probability q , simulates the system in contact with a thermal reservoir at temperature T and favors the lowest energy state of the system. In contrast, the two-spin flip dynamic, acting with probability $1 - q$, introduces an external energy flux into the system, favoring the highest energy state of the system.

In previous studies on the competition between these reactive dynamics using the two-dimensional Ising model, both on regular [15, 16] and complex [17, 18] networks, very similar phase diagrams were found. For low values of q , an antiferromagnetic phase almost independent of temperature is observed. As q increases, a second-order phase transition leads to the paramagnetic phase. However, with further increases in q , for low temperature values, the system transitions continuously back to an ordered phase, the ferromagnetic phase. This process reflects the self-organization of the system.

However, no studies have yet explored the competition between these dynamics in continuous-spin-state models. Thus, the objective of the present work is to implement the competition between one- and two-spin flip dynamics in the Ising, XY , and Heisenberg models on a simple cubic lattice, keeping the lattice unchanged. By focusing on variations in the magnetic models, we aim to verify whether the self-organization phenomenon and the phase diagram topology observed in previous studies persist under these new conditions.

This article is organized as follows: In Section II, we provide details about the Monte Carlo method (MC), the thermodynamic quantities of interest, and the scaling relations for each of them. The results are discussed in Section III, including the phase diagram and description of the second-order phase transitions. Finally, in Section IV, we present the conclusions drawn from the study.

* rafaeldumer@fisica.ufmt.br

† mgodoy@fisica.ufmt.br

II. MODEL AND METHOD

The interaction energy between spins is defined by the Hamiltonian model in the following form:

$$\mathcal{H} = - \sum_{\langle i,j \rangle} \{ J_{\perp} (S_i^x S_j^x + S_i^y S_j^y) + J_{\parallel} (S_i^z S_j^z) \}, \quad (1)$$

where the summation runs over all pairs of nearest neighbors on a regular simple cubic lattice, and the spins are treated as three-component vectors, with $|\mathbf{S}_i| = 1$. In the special case where $J_{\perp} = 0$ and $J_{\parallel} = 1$, the model reduces to the Ising model, while for $J_{\parallel} = 0$ and $J_{\perp} = 1$, it corresponds to the XY model. For the most general case, where $J_{\perp} = J_{\parallel} = 1$, the system represents the 3D isotropic Heisenberg model.

We have simulated the system specified by the Hamiltonian in Eq. (1), employing MC simulations. We always assumed periodic boundary conditions. Starting from the random initial state, a new spin configuration is generated following the Markov process: for a given competition probability q , temperature T e system size N , we randomly select a site on the lattice, \mathbf{S}_i , and generate a random number ξ between zero and one. If $\xi \leq q$, one-spin flip dynamics is chosen to simulate the system in contact with a heat bath. In this case, we randomly choose a new state for \mathbf{S}_i , which is accepted according to the Metropolis prescription [19]:

$$W(\mathbf{S}_i \rightarrow \mathbf{S}'_i) = \begin{cases} e^{(-\Delta E_i/k_B T)} & \text{if } \Delta E_i > 0 \\ 1 & \text{if } \Delta E_i \leq 0 \end{cases}, \quad (2)$$

where ΔE_i is the change in energy, based in Eq. (1), after flipping the spin \mathbf{S}_i , and k_B is the Boltzmann constant. With this transition rate, the new state is accepted if $\Delta E_i \leq 0$, but if $\Delta E > 0$ the state can still be accepted if, upon generating a random number ξ_1 between zero and one, it is less than or equal to the Boltzmann factor $\exp(-\Delta E_i/k_B T)$. On the other hand, if $\xi > q$, two-spin flip dynamics is chosen to simulate the system subjected to an external energy flux. In this case, we also randomly select one of the nearest neighbors of \mathbf{S}_i , \mathbf{S}_j . Here, both spins have their states altered randomly, and these new states are accepted with the following rate:

$$W(\mathbf{S}_i \mathbf{S}_j \rightarrow \mathbf{S}'_i \mathbf{S}'_j) = \begin{cases} 0 & \text{if } \Delta E_{ij} \leq 0 \\ 1 & \text{if } \Delta E_{ij} > 0 \end{cases}, \quad (3)$$

where ΔE_{ij} is the energy difference resulting from the change in spin states. With this dynamic, we observe that the change is only accepted if it increases the energy of the system, as expected for a system subjected to an external energy flux.

Repeating the Markov process N times constitutes one Monte Carlo Step (MCS). We allowed the system to evolve for 10^5 MCS to reach a stationary state, for all lattice sizes. To calculate the thermal averages of the quantities of interest, we conducted an additional 9×10^5 MCS.

The statistical errors were calculated using the Bootstrap method [20].

The measured thermodynamic quantities in our simulations are: magnetization per spin m_L^F , staggered magnetization m_L^{AF} , magnetic susceptibility χ_L and reduced fourth-order Binder cumulant U_L :

$$m_L^F = \sqrt{(m_x^F)^2 + (m_y^F)^2 + (m_z^F)^2}, \quad (4)$$

$$m_L^{AF} = \sqrt{(m_x^{AF})^2 + (m_y^{AF})^2 + (m_z^{AF})^2}, \quad (5)$$

$$\chi_L = \frac{N}{k_B T} \left[\langle m_L^2 \rangle - \langle m_L \rangle^2 \right], \quad (6)$$

$$U_L = 1 - \frac{\langle m_L^4 \rangle}{3 \langle m_L^2 \rangle^2}, \quad (7)$$

where $\langle \dots \rangle$ representing the thermal average over the MCS in the stationary state, and m_L can be either m_L^F or m_L^{AF} . We define:

$$m_{\alpha}^F = \frac{1}{N} \left\langle \sum_{i=1}^N S_i^{\alpha} \right\rangle, \quad (8)$$

$$m_{\alpha}^{AF} = \frac{1}{N} \left\langle \sum_{i=1}^N (-1)^{a+b+c} S_i^{\alpha} \right\rangle, \quad (9)$$

where α can be x, y or z , and $a + b + c$ is the sum of the spatial components of the position of S_i^{α} on the simple cubic lattice.

Near the critical point, the Eqs. (4), (5), (6) and (7) obey the following finite-size scaling relations [21]:

$$m_L = L^{-\beta/\nu} m_0(L^{1/\nu} \epsilon), \quad (10)$$

$$\chi_L = L^{\gamma/\nu} \chi_0(L^{1/\nu} \epsilon), \quad (11)$$

$$U_L' = L^{1/\nu} \frac{U_0'(L^{1/\nu} \epsilon)}{\Gamma_c}, \quad (12)$$

where $\epsilon = (\Gamma - \Gamma_c)/\Gamma_c$, and Γ can be T or q . Thus, β , γ , and ν are the critical exponents related the magnetization, susceptibility and correlation length, respectively. The functions $m_0(L^{1/\nu} \epsilon)$, $\chi_0(L^{1/\nu} \epsilon)$ and $U_0(L^{1/\nu} \epsilon)$ are the scaling functions.

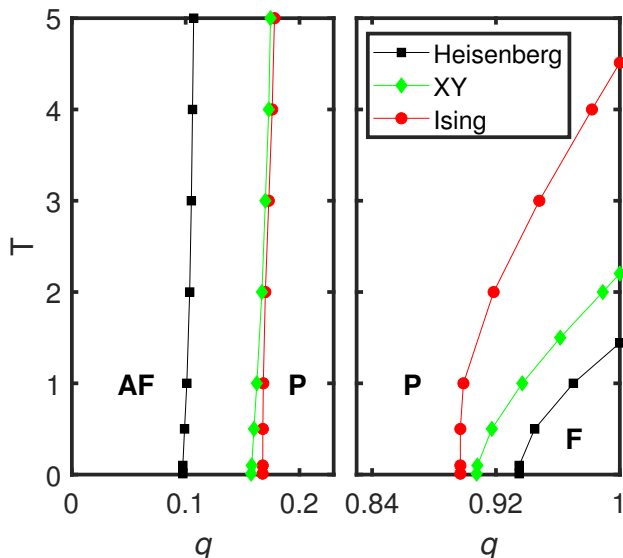


Figure 1. Phase diagram of the Ising, XY, and Heisenberg models, of temperature T versus competition parameter q on a simple cubic lattice. There are three phases: antiferromagnetic AF , ferromagnetic F and paramagnetic P . The solid lines serve only as visual guides for the second-order phase transition points. The statistical errors are smaller than the size of the symbols.

III. NUMERICAL RESULTS AND DISCUSSION

For low values of q , there is a high external energy flux into the system, which drives it to the highest energy state, the antiferromagnetic (AF) phase. However, as this energy flux decreases, neither of the dynamics is favored, leading the system to a disordered state characterized by the paramagnetic (P) phase. At high values of q , the dynamics simulating the system in contact with a thermal reservoir dominate, and magnetic ordering is once again observed at low temperatures, resulting in the ferromagnetic (F) phase, characteristic of the lowest energy state.

In this context, we constructed the phase diagram of the system, temperature T as a function of competition parameter q , where the three phases, AF , P , and F , are identified, as shown in Fig. 1. This figure presents the phase diagram for the models studied in the present work: Ising, XY , and Heisenberg.

We observe that when the two-spin flip dynamics dominate the system, i.e., at low q values, the system reaches its highest energy state, the AF phase. However, as q increases, a second-order phase transition leads to the disordered state, the P phase. Further increasing q causes the strong dominance of the one-spin flip dynamics, which continuously organizes the system into its lowest energy state, the F phase. Unlike the AF phase, the F phase is strongly temperature-dependent and occurs only at low T values.

In the phase diagram shown in Fig. 1, we observed

that the topology of the ordered phases remains practically unchanged regardless of the model being considered. The only difference between the ordered phases lies in the regions they occupy. As the spin degrees of freedom increase in the model, they become more influenced by the thermal fluctuations, which facilitates magnetic disordering. Consequently, the lowest temperature or less competition between the dynamics is required to transition into the disordered phase when dealing with models featuring higher spin degrees of freedom.

In addition to the characteristic topology of systems subjected to competing one- and two-spin flip dynamics, we also observed the phenomenon of self-organization in the studied models here. This self-organization manifests through the transitions between the ordered phases in the system. At low values of q , the system resides in the AF phase and when q increases, we observe a phase transition to the P phase. On the other hand, at high values of q , we observe a phase transition again to an ordered phase, the F phase. This behavior indicates that, beyond being independent of the lattice structure, as shown in previous studies [17, 18], the magnetic model subjected to these reactive dynamics retains its phase transition characteristics unchanged.

One way to identify the phase transition in the system is through the Binder cumulant curves [21, 22]. This method works because, at the critical point, the cumulant is independent of the system size. Thus, for curves corresponding to different system sizes L , the point where they intersect is identified as the phase transition point. Moreover, if the curves exhibit continuous behavior and only take positive values, they indicate a second-order phase transition. In this context, we present the Binder cumulant curves associated with the order parameter in the system for the three studied models and for several lattice sizes L , can be seen in Fig. 2.

In Fig. 2(a), we exhibit the Binder cumulant curves for the Ising model during the transition from the AF to the P phase and in Fig. 2(b) we have the curves for the same model corresponding to the transition from the P to the F phase. Similarly, in Figs. 2(c) and (d), the cumulant curves for the XY model are shown for the transitions from the AF to the P phase and from the P to the F phase, respectively. Finally, in Figs. 2(e) and (f) are displayed the cumulant curves for the Heisenberg model, also corresponding to the $AF - P$ and $P - F$ phase transitions, respectively. In all these figures, we observe the characteristic behavior of second-order phase transitions, along with the critical points, q_c , identified by the intersection of the curves at a fixed temperature of $T = 1.0$.

With well-defined critical points, we can more easily calculate the critical exponents of the system using the scaling relations from Eqs. (10), (11), and (12), which are valid near the criticality. To estimate the exponents, we take the values of the quantities near the critical point as a function of the linear lattice size L , plotted on a graph with logarithmic axes. The resulting curve exhibits a

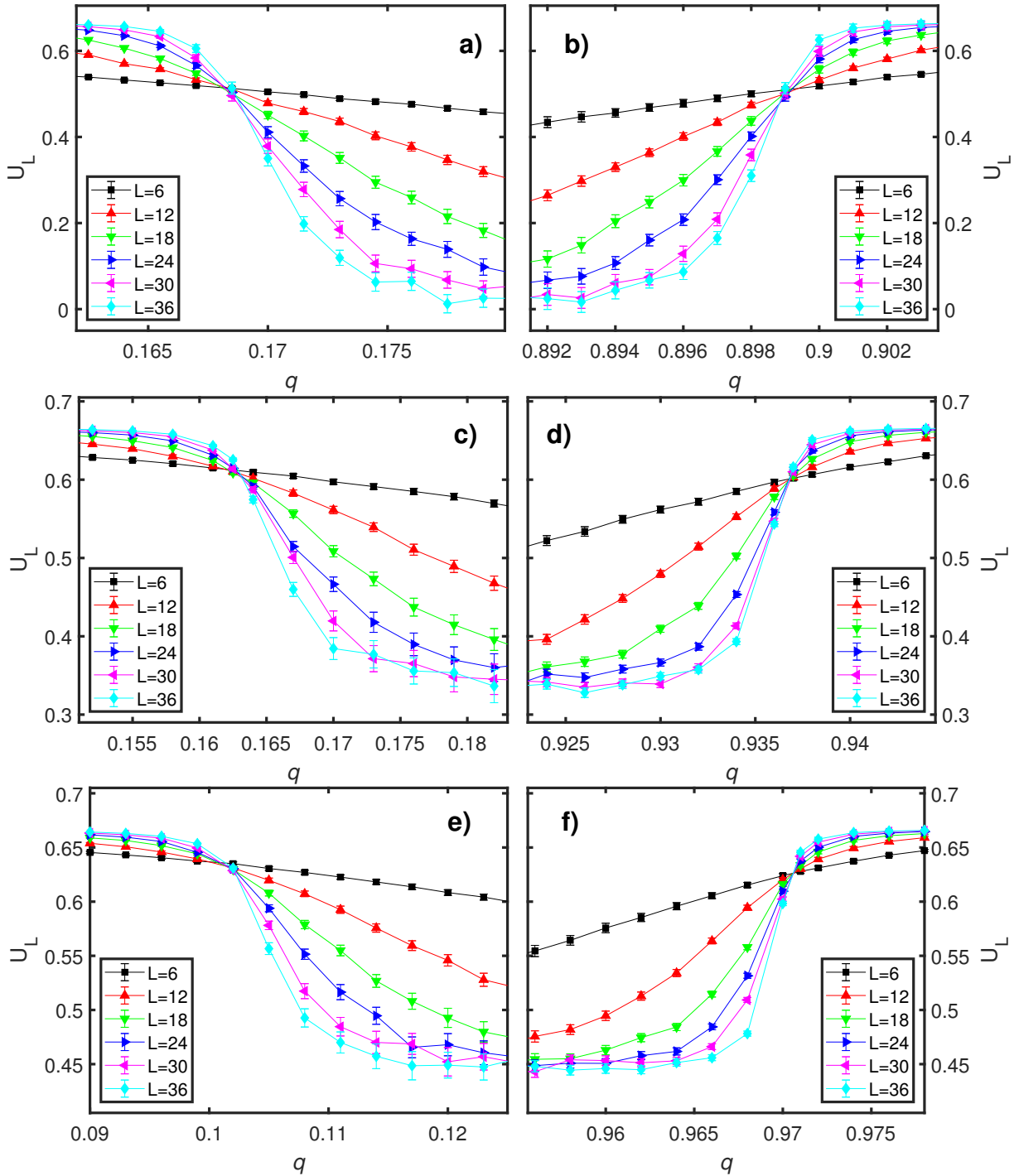


Figure 2. On the left, Binder cumulant curves at the transition from the AF to the P phases, while on the right, these curves correspond to the transition from the P to the F phases, for different lattice sizes L , as displayed in the figures. The (a) and (b) panels are results obtained for the Ising model, (c) and (d) for the XY model, (e) and (f) for the Heisenberg model. Here, the temperature is fixed for $T = 1.0$.

linear behavior, where the slope gives us the ratios of the critical exponents. From the m_L curves, based in Eq. (10), we obtain the ratio $-\beta/\nu$; from the χ_L curves, based in Eq. (11), the slope returns γ/ν . From the derivative of the Binder cumulant near the critical point, U'_L , we es-

timate the correlation length exponent $1/\nu$, based in Eq. (12). The linear fit of these thermodynamic quantities and the critical exponent estimates are shown in Fig. 3. In Fig. 3(a), we present the curves for the Ising model and in Figs. 3(b) and 3(c) we display the curves for the

XY and Heisenberg models, respectively.

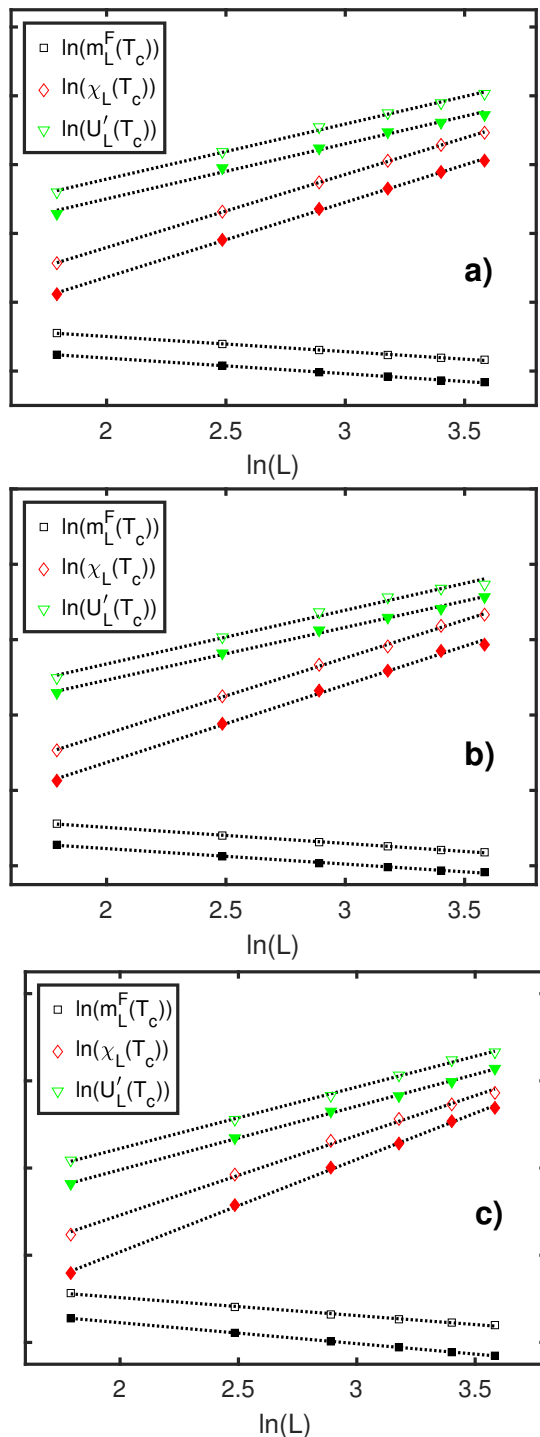


Figure 3. Linear fitting of the thermodynamic quantities near the critical point as a function of the linear lattice size L , in a graph with logarithmic scales on both axes. In (a), these curves correspond to the Ising model, in (b) the curves are obtained for the XY model, and in (c) for the Heisenberg model.

To support these estimates, we can use data collapse for the m_L and χ_L curves. With data collapse, we aim to obtain the forms of the scaling functions m_0 and χ_0 using curves of different lattice sizes L . This is possible because near the critical point if we use the correct critical point and critical exponents in the scaling functions from Eqs. (10) and (11), the result is a single curve, independent of the system size. To do this, we isolate the scaling function by plotting $m_L L^{\beta/\nu}$ and $\chi_L L^{-\gamma/\nu}$ as a function of $L^{1/\nu}\epsilon$, as shown in Fig. 4. In this case, we verify the validity of the obtained critical exponents, as the curves with different system sizes collapse into a single curve, representing the scaling functions. In Fig. 4(a), we present the collapsed curves for the transition from the AF to the P phase in the Ising model and in Fig. 4(b) we have shown the collapsed curves for the transition from the P to the F phase in the same model. Meanwhile, Fig. 4(c) displays the curve collapse for the XY model during the $AF - P$ phase transition, and Fig. 4(d) for the $P - F$ phase transition. Lastly, in Figs. 4(e) and (f), we present the collapsed curves for the Heisenberg model, corresponding to the AF to P and P to F phase transitions, respectively.

In order to qualitatively compare the critical exponents obtained in this work with those reported in the literature, we present Fig. 5. This figure shows the exponents along with their respective statistical errors, compared with the most precise results for the exponents of the Ising [23], XY [24], and Heisenberg [25] models on a simple cubic lattice under thermodynamic equilibrium.

From this comparison, we observe that the critical exponents obtained in this study slightly deviate from those in the literature. However, considering the statistical error margins inherent to the Metropolis algorithm, the values align with the known exponents. Thus, we conclude that the models in the non-equilibrium regime also preserve the system's universality class, both for the AF and F phase transitions.

IV. CONCLUSIONS

In this work, we studied the Ising, XY , and Heisenberg models on a simple cubic lattice evolving toward a stationary state through the competition between one- and two-spin flip dynamics. With probability q , the system relaxes to its lowest energy state, as it simulates contact with a heat bath at temperature T via one-spin flip dynamics. Conversely, with probability $1 - q$, the system evolves toward a higher energy state due to an external energy flux, governed by two-spin flip dynamics. We constructed the phase diagram of the system, plotting T as a function of q , which revealed three phases: antiferromagnetic AF , paramagnetic P , and ferromagnetic F . At low values of q , where a high external energy flux is

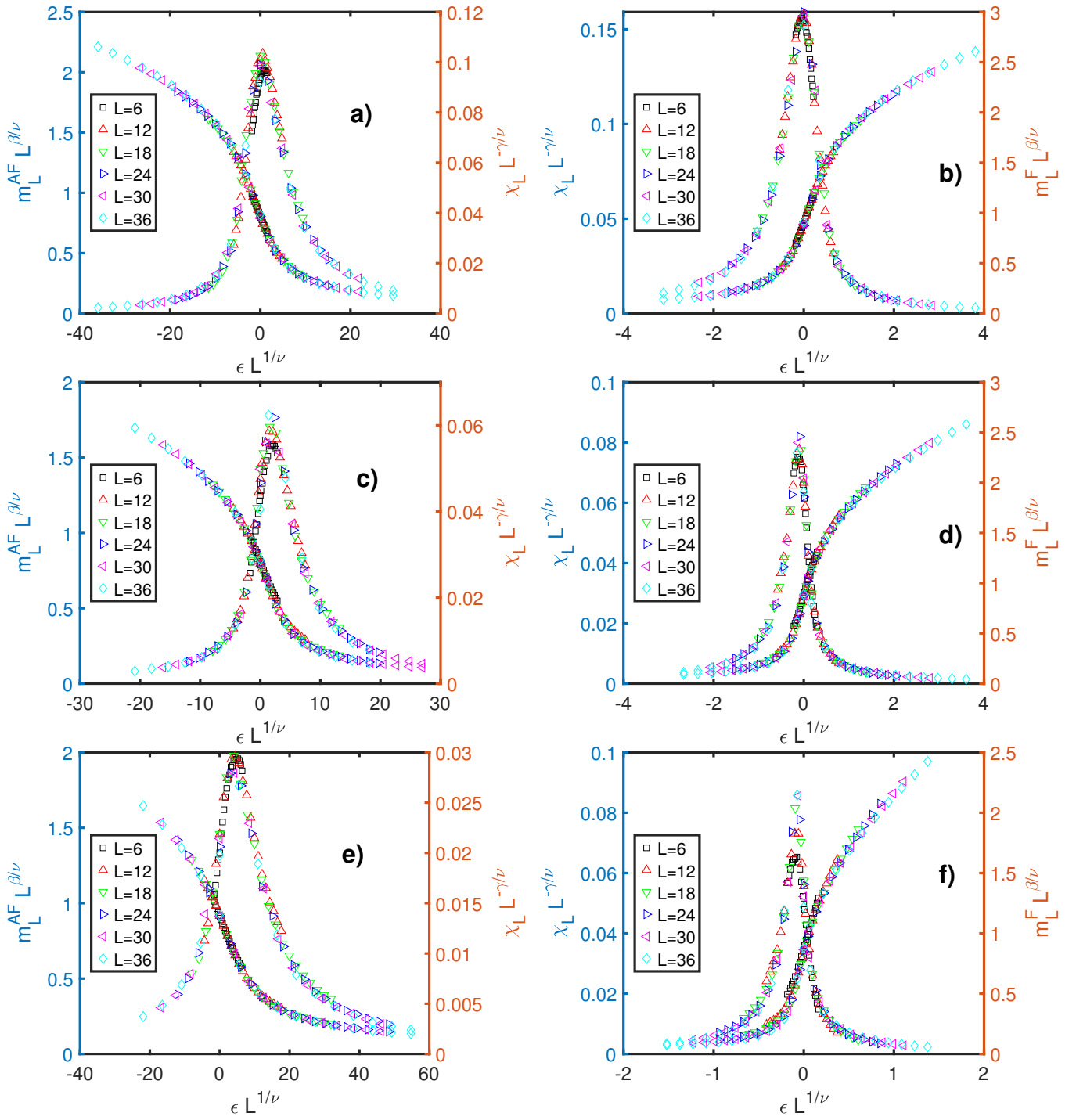


Figure 4. On the left, we have the curves corresponding to the data collapse of magnetization and magnetic susceptibility at the transition from the *AF* to the *P* phases, while on the right, these curves correspond to the transition from the *P* to the *F* phases, for different lattice sizes L , as displayed in the figures. The (a) and (b) panels are the data collapse for the Ising model, (c) and (d) for the XY model, (e) and (f) for the Heisenberg model. Here, the temperature is fixed for $T = 1.0$.

introduced into the system due to two-spin flip dynamics, we observed the system in its highest energy state, the *AF* phase. As q increases, the system continuously transitions to the disordered *P* phase. Further increasing q leads to a regime where one-spin flip dynamics dominate

the system, allowing a return to an ordered phase, the *F* phase, at low values of T . This phase corresponds to the lowest energy state. We found that the topology of the phase diagram remains unchanged regardless of the magnetic model studied, indicating that it is determined

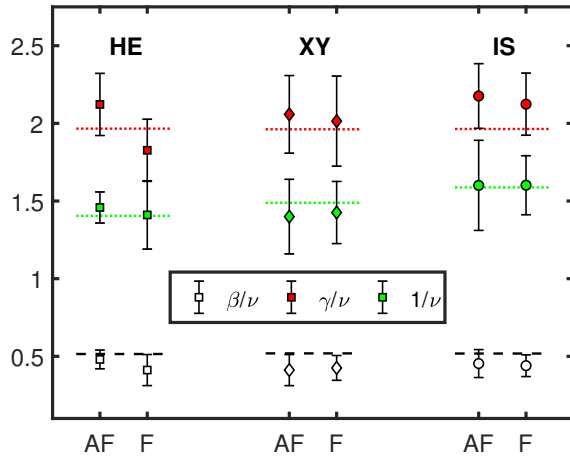


Figure 5. Relation of the critical exponents obtained for the Ising (IS), XY, and Heisenberg (HE) models, at the transition from the AF to the P phases, and from the P to the F phases, as shown on the horizontal axis. The horizontal lines correspond to known results from the literature for these exponents [23–25].

by the reactive dynamics used. The differences in the diagram between models lie only in the size of the ordered phases: models with higher spin-state degrees of freedom exhibit smaller ordered phase regions in the diagram. Beyond phase transitions, we also calculated the system's critical exponents and compared them with established results in the literature. This comparison confirmed that the non-equilibrium regime did not alter the universality class of the studied models.

-
- [1] E. Ising, Z. Physik 31, 253 (1925).
[2] W. Heisenberg, Z. Physik 49, 619 (1928).
[3] J. M. Kosterlitz, and D. J. Thouless, J. Phys. C 6, 1181 (1973).
[4] N. D. Mermin, and H. Wagner, Phys. Rev. Lett. 17, 1133 (1966).
[5] G. Nicolis, and I. Prigogine, *Self-Organization in Nonequilibrium Systems* (Wiley, New York, 1977).
[6] J. J. Tyson. Biochem. J. 479, 185 (2022).
[7] T. Vicsek, and A. Zafeiris, Phys. Rep. 517, 71 (2012).
[8] I. M. De la Fuente, *et al.*, Front. Genet. 12, 644615 (2021).
[9] D. Helbing, Rev. Mod. Phys. 73, 1067 (2001).
[10] T. Tomé and M. J. de Oliveira, Phys. Rev. A 40, 6643 (1989).
[11] Y.-q. Ma, and J.-w. Liu, Phys. Let. A, 238, 159 (1998).
[12] T. Tomé, M. J. de Oliveira, and M. A. Santos, J. Phys. A: Math. Gen. 24, 3677 (1991).
[13] A. Szolnoki, Phys. Rev. E 62, 7466 (2000).
[14] J. W. Gibbs, *Elementary Principles in Statistic Mechanics* (Yale Universality Press, New Haven, CT, 1902).
[15] M. Godoy and W. Figueiredo, Phys. Rev. E 66, 036131 (2002).
[16] M. Godoy and W. Figueiredo, Phys. Rev. E 65, 026111 (2002).
[17] R. A. Dumer and M. Godoy, Phys. Rev. E 107, 044115 (2023).
[18] R. A. Dumer and M. Godoy, Physica A 626, 129111 (2023).
[19] N. Metropolis, A. W. Rosenbluth, M. N. Rosenbluth, and A. H. Teller, J. Chem. Phys. 21, 1087 (1953).
[20] M. E. J. Newman and G. T. Barkema. *Monte Carlo Methods in Statistical Physics*, 1st ed. (Oxford University Press, New York, EUA, 1999).
[21] L. Böttcher and H. J. Herrmann. *Computational Statistical Physics*, 1st ed. (Cambridge University Press, New York, EUA, 2021).
[22] S.-H. sai, S.R. Salinas, Braz. J. Phys. 28, 1 (1998).
[23] A. M. Ferrenberg, J. Xu, and D. P. Landau, Phys. Rev. E 97, 043301 (2018).
[24] M. Campostrini, M. Hasenbusch, A. Pelissetto, and E. Vicari, Phys. Rev. B 74, 144506 (2006).
[25] G. Albuquerque Silva, A. R. Bergeron, J. A. Plascak, and D. P. Landau, Phys. Rev. E 109, 064113 (2024).

ACKNOWLEDGMENTS

This work has been supported by the Conselho Nacional de Desenvolvimento Científico e Tecnológico (CNPq), Brazil (Process No. 140141/2024-3).